Research Article

Lubomír Lapčík*, Martin Vašina*, Barbora Lapčíková, Michal Staněk, Martin Ovsík, and Yousef Murtaja

Study of the material engineering properties of high-density poly(ethylene)/perlite nanocomposite materials

https://doi.org/10.1515/ntrev-2020-0113
received December 6, 2020; accepted December 19, 2020

Abstract: This paper was focused on application of the perlite mineral as the filler for polymer nanocomposites in technical applications. A strong effect of the perlite nano-filler on high-density poly(ethylene) (HDPE) composites' mechanical and thermal properties was found. Also found was an increase of the Young's modulus of elasticity with the increasing filler concentration. Increased stiffness from the mechanical tensile testing was confirmed by the nondestructive vibrator testing as well. This was based on displacement transmissibility measurements by means of forced oscillation single-degree-of freedom method. Fracture toughness showed a decreasing trend with increasing perlite concentration, suggesting occurrence of the brittle fracture. Furthermore, ductile fracture processes were observed as well at higher filler concentrations by means of SEM analysis. There was also found relatively strong bonding between polymer chains and the filler particles by SEM imagining.

Keywords: perlite fillers, HDPE composites, mechanical testing, vibration damping, thermal analysis

*** Corresponding author: Lubomír Lapčík,** Department of Physical Chemistry, Faculty of Science, Palacky University, 17. Listopadu 12, 771 46, Olomouc, Czech Republic; Faculty of Technology, Tomas Bata University in Zlin, Nam. T.G. Masaryka 275, 760 01, Zlin, Czech Republic, e-mail: lapcikl@seznam.cz
*** Corresponding author: Martin Vašina,** Faculty of Technology, Tomas Bata University in Zlin, Nam. T.G. Masaryka 275, 760 01, Zlin, Czech Republic; VŠB-Technical University of Ostrava, Department of Hydromechanics and Hydraulic Equipment, Faculty of Mechanical Engineering, 17. Listopadu 15/2172, 708 33, Ostrava-Poruba, Czech Republic, e-mail: martin.vasina@vsb.cz
Barbora Lapčíková: Department of Physical Chemistry, Faculty of Science, Palacky University, 17. Listopadu 12, 771 46, Olomouc, Czech Republic; Faculty of Technology, Tomas Bata University in Zlin, Nam. T.G. Masaryka 275, 760 01, Zlin, Czech Republic
Michal Staněk, Martin Ovsík: Faculty of Technology, Tomas Bata University in Zlin, Nam. T.G. Masaryka 275, 760 01, Zlin, Czech Republic
Yousef Murtaja: Department of Physical Chemistry, Faculty of Science, Palacky University, 17. Listopadu 12, 771 46, Olomouc, Czech Republic

1 Introduction

Modification and recycling of polymers is an important part of the polymer research and applications [1–3]. Thermoplastics, such as polyethylene, can offer useful mechanical, chemical, electrical [4], and optical [5] properties, e.g., as the structural supporting components [6] and packaging materials [7]. Due to its low price per unit volume and unique physicochemical properties, it is globally the most used thermoplastic [8]. Poly(ethylene) is a semicrystalline polymer. It is classified based on its density. There are four different groups: high-density polyethylene (HDPE), low-density polyethylene (LDPE), linear low-density polyethylene (LLDPE), and very low-density polyethylene (VLDPE) [9]. Covalent bond between carbon atoms of the poly(ethylene) molecule is extremely stiff and strong similarly as in the diamond. Furthermore, poly(ethylene) chain has the smallest transversal cross-section compared to all polymers [10]. This is due to the lack of the presence of the pendant groups in its macromolecular structure. Therefore, the system of the unidirectional-oriented polyethylene chains has relatively high strong elements available per unit area capable to transmit high mechanical stresses. For this reason, the macroscopic mechanical strength of such structure is very high. Semiempirical estimations of the maximum strength of the polyethylene along its macromolecular chain vary in the range of 16–36 GPa. Theoretical calculations of the modulus of elasticity propose magnitudes from 180 to 340 GPa [10]. However, there was found increased risk of cavities formation at the nano-filler/polymer matrix interface in the HDPE

nanocomposites due to the difference in the Young's modulus of elasticity between the polymer matrix and the filler nanoparticles [11].

Moreover, the tensile properties of polymer fibers might be significantly affected by their fiber structure as found for polyacrylonitrile (PAN) membranes [12]. It was found that these decrease significantly with increasing the fiber orientation angle. The results also showed that the nanofiber membranes exhibited ductile fracture pattern.

The fundamental mechanisms governing the size-dependent mechanical behavior of different crystal structures were described in detail in [13], where the effects of fabrication process and current experimental techniques for micro and nano-compression were investigated as well. The influence of the surface effect on the properties of the nano-scale sample is directly associated with the surface to volume ratio.

Mineral fillers were used as an additive in polymer nanocomposites [14], silicon rubber [15], and in combination with the polyvinyl alcohol fibers/nano-SiO_2 fillers as reinforced cementitious composites [16] in the last decade. At the present, mineral nano-fillers were used as friction reducing additives for improving tribological performance and wear resistance of HDPE [17]. HDPE-nanoclay composites were also used in the additive manufacturing by means of the 3D printing technology, where increase in Young's modulus of elasticity with increasing nanoclay concentration was found [18]. It was found that the net effect of the nano-fillers on the wear resistance was due to the combination of different abilities of the nano-fillers to modify the tensile and compressive mechanical properties of polymers. These were manifested in the observed surface hardness and ductility of the nano-composite, contributed by the nano-fillers to the friction coefficient and the creation of the transfer film [17]. The effect of incorporating nano-fillers into the thermoplastic polymer network results in the improvement of the physicochemical and mechanical characteristics such as low air permeability [19], improved mechanical strength, modulus of elasticity, and stiffness [20–22]. That is why, now, the research focused on composites containing inorganic fillers is important. Perlite powder is an essential material for the application of thermal and acoustic insulation materials [23]. Perlite is the mineral formed by the cooling of volcanic eruptions. It is composed of SiO_2, Al_2O_3, K_2O, Na_2O, and water. Depending on its origin, perlite may contain also TiO_2, CaO, and MgO. When subjected to thermal treatment, natural perlite particles expand up to 20 times in volume, due to the water vaporization [24]. Expanded perlite was also found as an effective sound-absorbing material due to its open pore structure [25]. When sound waves of a certain wavelength enter such pores, they effectively absorb the acoustic energy. Applications of polyethylene prepared with the addition of perlite were reported elsewhere [25]. It was found that perlite enhanced the thermal stability and sound absorption coefficients of polyesters.

Polymer matrix modification, its crystallinity degree, type of reinforcement, filler/matrix adhesion quality [26], filler particles size, etc. influence physicochemical, thermal, and mechanical properties of the final composites [27,28]. That is why, detailed understanding of the effect of the polymer matrix and the filler particles on the overall composite performance in consumer technical products, e.g., at the mechanical deformation loads both static and dynamic, is of scientific and practical importance. For that reason, this paper is focused on combination of the destructive and nondestructive mechanical testing [29] and thermal analysis in combination with SEM imagining for perlite/HDPE composites analysis.

2 Materials

High-density poly(ethylene) (HDPE) type 25055E (The Dow Chemical Company, USA) was used in the form of white pellets (lot. No. 1I19091333). As the filler particles, the inorganic volcanic glass mineral perlite (Supreme Perlite Company, USA) was applied (d_{50} = 447 nm diameter, density 1.10 g/cm^3) [30]. Perlite filler moisture content was 0.1 wt%. There were prepared 150 composites samples (dog bone shape for tensile testing, Charpy's pendulum, and vibrator testing) of virgin HDPE and 5, 10, and 15 wt% of inorganic filler concentrations of perlite/HDPE composites. Composite samples were prepared by means of the injection molding technology on the injection molding machine Arburg Allrounder type 420 C (Germany). Applied processing temperature ranged from 190 to 220°C, mold temperature 30°C, injection pressure 60 MPa, and injection rate 20 mm/s [31]. Extrusion machine Scientific was used for virgin and composite samples extrusion at the processing temperature ranging from 136 to 174°C, L/D = 40.

3 Methods

3.1 Scanning electron microscopy

Scanning electron microscopy (SEM) images were captured using a Scanning Electron Microscope Hitachi SU

6600 (Japan). The source of the electrons is Schottky cathode. This microscope has the resolution in secondary electron mode (SE) 1.3 nm and in back scattered electrons (BSE) 3 nm. For these images, the SE and an accelerating voltage of 5 kV were used. The distance between sample and detector was 6 mm. Studied materials were placed on double-sided carbon tape on aluminium holder.

3.2 Thermal analysis

For perlite/HDPE nanocomposites, virgin HDPE thermogravimetry (TG), and differential thermal analysis (DTA), experiments were performed on a simultaneous DTA-TG apparatus (Shimadzu DTG 60, Japan). Measurements were performed at a heat flow rate of 10°C/min in a dynamic nitrogen atmosphere (50 ml/min) at the temperature range from 30 to 550°C. The crystallinity (w_C) of the nanocomposites was calculated according to the formula (1) [32,33]:

$$w_C = \frac{\Delta H_m}{\Delta H_m^0} \times 100 \tag{1}$$

where: $\Delta H_m^0 = 293\ J\ g^{-1}$ is heat of fusion for 100% crystalline material HDPE, heated at rate of 10°C/min [32,34], and ΔH_m ($J\ g^{-1}$) is measured heat of fusion.

3.3 Uniaxial tensile testing

Tensile testing of injection-molded specimens was performed on a Zwick 1456 multipurpose tester (Germany). The measurements were realized according to CSN EN ISO 527-1 and CSN EN ISO 527-2 standards [35]. Samples were strained at room temperature up to break at the test speeds of 50, 100, and 200 mm/min. From the stress–strain dependencies, Young's modulus of elasticity and elongation at break were calculated. Each experiment was repeated 10× at the ambient temperature of 22°C and average values and standard errors were calculated.

3.4 Charpy impact testing

Impact tests were performed on Zwick 513 Pendulum Impact Tester (Germany) according to the CSN EN ISO 179-2 standard with the drop energy of 25 J.

3.5 Displacement transmissibility measurement

The material's ability to damp harmonically excited mechanical vibration of single-degree-of freedom (SDOF) systems is characterized by the displacement transmissibility T_d, which is expressed by the equation [36,37]:

$$T_d = \frac{y_2}{y_1} = \frac{a_2}{a_1}, \tag{2}$$

where: y_1 is the displacement amplitude on the input side of the tested sample and y_2 is the displacement amplitude on the output side of the tested sample, a_1 is the acceleration amplitude on the input side of the tested sample and a_2 is the acceleration amplitude on the output side of the tested sample.

Generally, there are three different types of mechanical vibration depending on the value of the displacement transmissibility, namely, resonance ($T_d > 1$), undamped ($T_d = 1$), and damped ($T_d < 1$) vibration [37].

The displacement transmissibility of a spring-mass-damper system, which is described by spring (stiffness k), damper (damping coefficient c), and mass m, is given by the following equation [36–38]:

$$T_d = \sqrt{\frac{k^2 + (c \times \omega)^2}{(k - m \times \omega^2)^2 + (c \times \omega)^2}} = \sqrt{\frac{1 + (2\zeta \times r)^2}{(1 - r^2)^2 + (2\zeta \times r)^2}} \tag{3}$$

where: ζ is the damping ratio and r is the frequency ratio, which are expressed by the formulas [39,40]:

$$\zeta = \frac{c}{2\sqrt{k \times m}}, \tag{4}$$

$$r = \frac{\omega}{\omega_n} = \frac{\omega}{\sqrt{k/m}}, \tag{5}$$

where: ω is frequency of oscillation and ω_n is the natural frequency [41,42]. Under the condition $dT_d/dr = 0$ in the equation (3), it is possible to find the frequency ratio r_0, at which the displacement transmissibility has its maximum value [36]:

$$r_0 = \frac{\sqrt{\sqrt{1 + 8\zeta^2} - 1}}{2\zeta}. \tag{6}$$

It is evident from the equation (6) that the local extreme of the displacement transmissibility is generally shifted to lower values of the frequency ratio r with the increasing damping ratio ζ (or with the decreasing material stiffness k). The local extrema (i.e., the maximum

value of the displacement transmissibility T_{dmax}) is obtained at the frequency ratio r_0 from the equation (6).

The mechanical vibration damping testing of the investigated materials was performed by the forced oscillation method. The displacement transmissibility T_d was experimentally measured using the BK 4810 vibrator in combination with a BK 3560-B-030 signal pulse multi-analyzer and a BK 2706 power amplifier at the frequency range from 2 to 3,200 Hz. The acceleration amplitudes a_1 and a_2 on the input and output sides of the investigated specimens were evaluated by means of BK 4393 accelerometers (Brüel & Kjær, Nærum, Denmark). Measurements of the displacement transmissibility were performed for three different inertial masses m (i.e., ranging from 0, 90, and 500 g), which were positioned on the upper side of the periodically tested samples. The tested block article dimensions were (60 × 60 × 3) mm (length × width × thickness). Each measurement was repeated 5 times at an ambient temperature of 23°C.

4 Results and discussion

As known from earlier studies [35], applied inorganic nano/micro particles are used as functional fillers modulating elastoplastic behavior of polymer composites. It was found that dominating factors responsible for controlled mechanical response patterns of the composites are mainly the physicochemical properties of the applied polymer base matrix (e.g., HDPE, low-density poly(ethylene) (LDPE), linear low-density poly(ethylene) (LLDPE), etc.) and the properties of the filler particles (e.g., their uniformity, shape, diameter, and surface chemistry). Other factors, which should be taken into account, are the ratio of the amorphous/crystalline regions of the polymer matrix and the quality of the interface adhesion between filler particles and the polymer matrix [9].

SEM images of the perlite micro/nano-filler particles are shown in Figure 1a and b.

There is an evidence confirming their porous internal structure as shown in Figure 1a. As it is well-known from the literature [30,43,44], the porous micro/nano structures of the fillers or the whole composite articles are directly affecting their sound absorption, vibration damping properties as well as their dynamic mechanical properties [31,45,46].

Typical filler concentration dependencies of the Young's modulus of elasticity (E) of the studied perlite/HDPE composites are shown in Figure 2.

They were characteristic with the gradual increase of the E with the increasing perlite concentration for all deformation rates under study (50, 100, and 200 mm/min). There was observed approximately 37% increase in E for 15 wt% perlite concentration compared to the virgin HDPE. This triggered substantial increase of the materials' stiffness. However, this phenomenon was accompanied with the corresponding exponential decrease of the observed elongation at break with the increasing filler concentration as shown in Figure 3.

There was confirmed increasing stiffness of the composite response to the applied uniaxial deformation with the increasing deformation rate as reflected by original elongation at break for the virgin polymer of 220% (50 mm/min deformation rate) changed to 70% (100 mm/min deformation rate) and to 45% (200 mm/min deformation rate). Interestingly, these differences were not much significant for higher concentrations of the filler exceeding 10 wt% perlite/HDPE composite matrices, suggesting lowered mobility of the poly(ethylene) macromolecular chains.

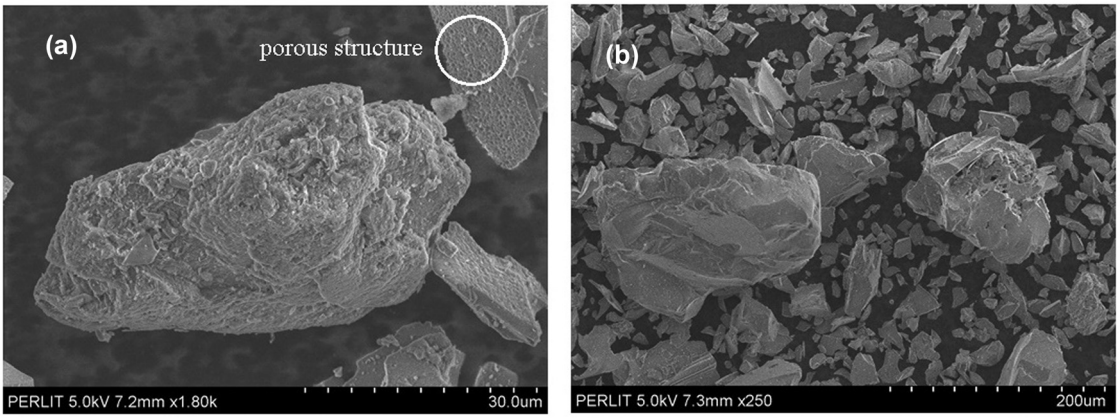

Figure 1: SEM image of the perlite micro/nano-filler.

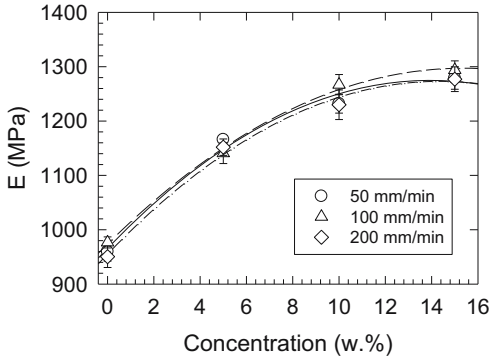

Figure 2: Young's modulus of elasticity (E) vs perlite filler concentration. Inset: applied deformation rates.

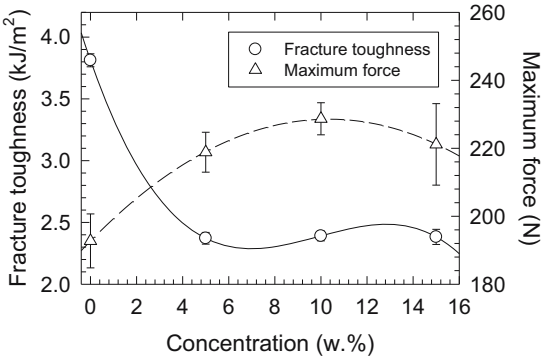

Figure 4: Fracture toughness and maximum force vs perlite filler concentration dependencies.

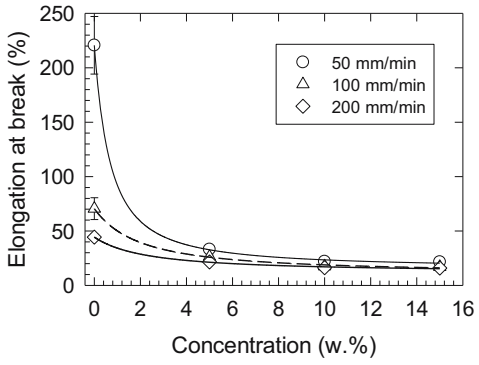

Figure 3: Elongation at break vs perlite filler concentration. Inset: applied deformation rates.

Results of the fracture mechanics measurements of the studied composites are shown in Figure 4.

There was found exponential decrease of the fracture toughness from 3.8 kJ/m^2 (virgin HDPE) to 2.4 kJ/m^2 for perlite/HDPE composites in the perlite concentration range from 5 to 15 wt%. As observed earlier during uniaxial tensile testing, mineral filler brought increase of the material stiffness to the composite matrix as reflected by the increasing modulus E with the increasing filler concentration. Also during impact fracture testing performed on Charpy pendulum, similar effect was confirmed, as reflected in Figure 4, by the increasing maximum force with the increasing filler concentration.

With respect to the proposed mechanical energy transfer mechanism, the SEM images shown in the Figure 5 clearly recognized plastically transformed polymer regions characteristic with the well-developed spurs and deformation bands typical for ductile fracture interface (Figure 5b–d) as well as brittle fracture regions as shown in Figure 5a and b.

Results of the dynamic mechanical testing of the studied composites by the forced oscillation method on vibrator device are shown in Figures 6 and 7.

Here (Figure 6), typical frequency dependencies of the displacement transmissibility demonstrated increased material stiffness with the increasing filler concentration as reflected by appearance of the first resonance frequency (f_{R1}) peak position (Table 1).

There was confirmed validity of the formula (6), where with increasing stiffness (or decreasing damping ratio) the f_{R1} peak position was shifted to the higher excitation frequencies. Obtained dynamic mechanical behavior was in excellent agreement with tensile testing measurements, where the E was increased with the increasing perlite concentration in the polymer composite matrix. It was also found that the f_{R1} was shifted to the lower excitation frequencies with the increasing inertial mass applied during vibrational measurements. This fact is in agreement with the formula (4), where the increasing inertial mass m leads to the lower natural frequency ω_n, thus to the lower f_{R1}. From the practical point of view, this method (vibration damping) allows nondestructive evaluation of the stiffness of the polymer nanocomposites in contrary to the destructive tensile or fracture tests.

Results of the thermal analysis are shown in Figure 8a and b and Table 2.

There was found a minor increase of the melting temperature from 137.4°C (virgin HDPE) to 141.6°C (15 wt% perlite/HDPE composite), indicating a stronger bonding between polymer chains and the filler particles. However, the crystallinity was decreased with the increasing perlite concentration from original 60.65 to 28.16%, suggesting perlite had no positive effect on HDPE crystallization as

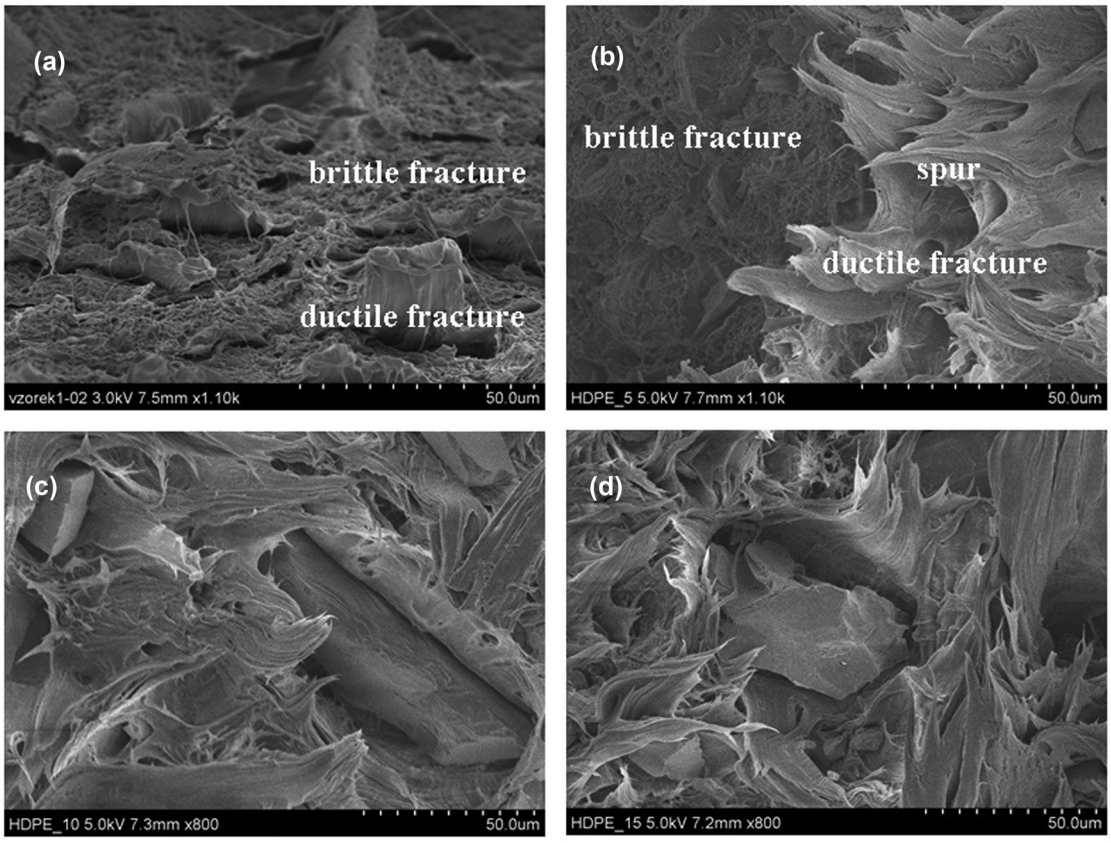

Figure 5: SEM images of the fracture surface after the tensile testing of the samples: (a) virgin HDPE, (b) 5 wt% perlite/HDPE composite, (c) 10 wt% perlite/HDPE composite, (d) 15 wt% perlite/HDPE composite. (50 mm/min applied deformation rate).

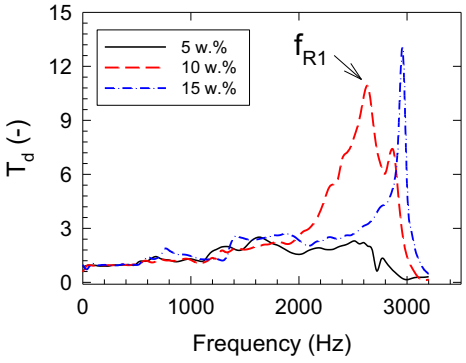

Figure 6: Frequency dependencies of the displacement transmissibility of the tested perlite/HDPE composites (Inset: perlite concentration) without inertial mass (m = 0 g).

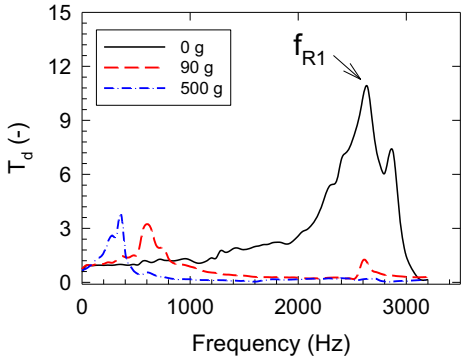

Figure 7: Frequency dependencies of the displacement transmissibility of the tested perlite/HDPE composites (Inset: inertial mass) of 10 wt% perlite concentrations.

was reported, e.g., for halloysite nanotubes filler [47]. It was found (Figure 8a) that the highest degradation rate was observed for 5 wt% composite; however, the lowest degradation rate was found for 15 wt% composite. All curves exhibited one single degradation step attributed to the radical random scission mechanism of polyolefin thermal decomposition [33]. Compared to the virgin HDPE, the onset of the degradation of 15 wt% perlite/HDPE composite was shifted to the lower value, where according to Cuadri *et al.* [33] the predominant chain scission provoked the formation of low-thermal stability compounds. The latter compounds were consecutively eliminated at lower temperatures.

Table 1: First resonance frequency f_{R1} and the corresponding maximum displacement transmissibility T_{dmax} of the investigated composites as induced by harmonically excited vibration; c – perlite concentration

c [wt%]	Quantity	Inertial mass (g)		
		0	90	500
5	f_{R1} [Hz]	1,614 ± 72	593 ± 26	341 ± 15
	T_{dmax} [–]	2.5 ± 0.2	3.1 ± 0.2	3.7 ± 0.3
10	f_{R1} [Hz]	2,627 ± 112	603 ± 25	346 ± 16
	T_{dmax} [–]	12.1 ± 0.9	3.3 ± 0.2	4.5 ± 0.4
15	f_{R1} [Hz]	2,944 ± 129	626 ± 28	396 ± 17
	T_{dmax} [–]	14.2 ± 1.1	4.6 ± 0.3	4.8 ± 0.4

Table 2: Results of the thermal analysis of the virgin HDPE and perlite/HDPE composites

c [wt%]	T_m [°C]	ΔH_m [J g^{-1}]	w_C [%]	T_A [°C]	T_D [°C]	TWL [%]
0	137.4	177.7	60.65	455	477.2	100.0
5	136.4	133.9	48.10	463.9	476.1	93.1
10	139.9	92.9	31.44	462.1	474.7	90.0
15	141.6	82.5	28.59	451.3	474.3	86.2

c – filler concentration, T_m – melting peak temperature, ΔH_m – heat of fusion, w_C – crystallinity, T_D – DTA peak of decomposition, T_A – starting point – intersection of extrapolated staring mass with the tangent applied to the maximum slope of the TG curve (decomposition behavior), TWL – total weight loss, ΔH_m endothermic process detected in the temperature range from 95 to 175°C for all samples.

5 Conclusions

It was found in this study that perlite mineral filler is strongly influencing mechanical and thermal properties of HDPE polymer nanocomposites. There was a confirmed gradual increase of the Young's modulus of elasticity accompanied with the corresponding decrease of the elongation at break with the increasing filler concentration. There was an observed 37% increase in the Young's modulus of elasticity for 15 wt% perlite concentration in comparison with the virgin HDPE. The observed increased stiffness from the tensile testing was confirmed by the nondestructive vibrator testing based on measurement of the displacement transmissibility during forced oscillation measurements. It was reflected by the shift of the first resonance frequency peak position to the higher excitation frequencies. Fracture toughness showed a decreasing trend with the increasing perlite concentration from 4 to 2.3 kJ/m^2, suggesting occurrence of the brittle fracture as well. However, there were observed regions of the ductile fracture processes at higher filler concentrations as found in SEM images. These were characteristic with the observed polymer deformation bands and spurs. It can be concluded that the perlite particles function as the stress concentrators in the complex composite matrix. There was found a minor increase of the melting temperature with the increasing filler concentration, indicating a stronger bonding between polymer chains and the filler particles.

Acknowledgments: This study was supported by the European Regional Development Fund in the Research Centre of Advanced Mechatronic Systems project, project number CZ.02.1.01/0.0/0.0/16_019/0000867. Authors LL and YM would like to express their gratitude for financing this research to the internal grant of Palacky University in Olomouc IGA_PrF_2020_022. Financial support to the author YM by Fischer scholarship of the Faculty of Science, Palacky University in Olomouc in 2020 year, is gratefully acknowledged as well. Special thanks to Dr. K. Čépe for SEM measurements (Palacky University in Olomouc).

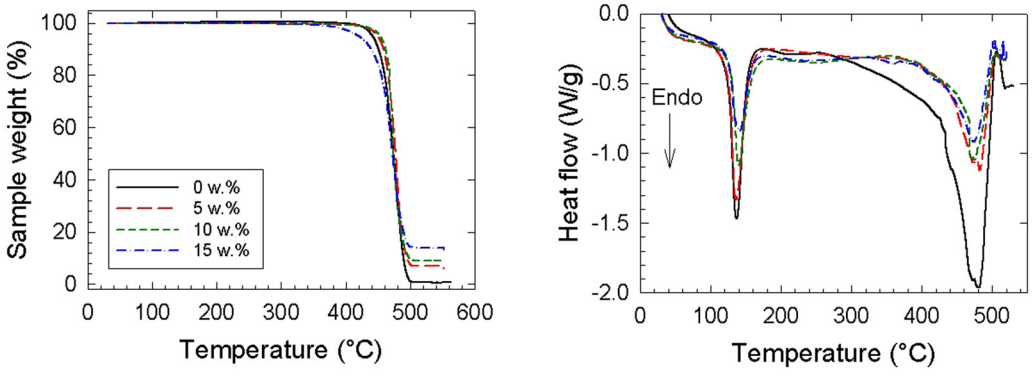

Figure 8: Results of the TGDTA thermal analysis of the studied perlite/HDPE composites. Inset: Perlite concentration.

Conflict of interest: The authors declare no conflict of interest regarding the publication of this paper.

References

[1] Lei M, Chen Z, Lu H, Yu K. Recent progress in shape memory polymer composites: methods, properties, applications and prospects. Nanotechnol Rev. 2019 Jan;8(1):327–51.

[2] Chamis CC. Polymer composite mechanics review – 1965 to 2006. J Reinf Plast Compos. 2007;26(10):987–1019.

[3] Singh N, Hui D, Singh R, Ahuja IPS, Feo L, Fraternali F. Recycling of plastic solid waste: a state of art review and future applications. Compos Part B Eng. 2017 Apr 15;115:409–22.

[4] Mora A, Verma P, Kumar S. Electrical conductivity of CNT/polymer composites: 3D printing, measurements and modeling. Compos Part B Eng. 2020 Feb 15;183:107600.

[5] Wang X, Xu P, Han R, Ren J, Li L, Han N, et al. A review on the mechanical properties for thin film and block structure characterised by using nanoscratch test. Nanotechnol Rev. 2019 Jan;8(1):628–44.

[6] Kenisarin MM, Kenisarina KM. Form-stable phase change materials for thermal energy storage. Renew Sustain Energy Rev. 2012 May;16(4):1999–2040.

[7] Gill YQ, Jin J, Song M. Comparative study of carbon-based nanofillers for improving the properties of HDPE for potential applications in food tray packaging. Polym Polym Compos. 2020 Oct;28(8–9):562–71.

[8] Sauter DW, Taoufik M, Boisson C. Polyolefins, a success story. Polymers. 2017 Jun;9(6):185.

[9] Krasny I, Lapcik L, Lapcikova B, Greenwood RW, Safarova K, Rowson NA. The effect of low temperature air plasma treatment on physico-chemical properties of kaolinite/polyethylene composites. Compos Part B Eng. 2014 Mar;59:293–9.

[10] Lapcik L, Raab M. Materials science II. Textbook. Zlin, Tomas Bata University in Zlin, 2nd edn. Zlin: Tomas Bata University in Zlin; 2004.

[11] Perchacz M, Rozanski A, Kargarzadeh H, Galeski A. Cavitation in high density polyethylene/Al2O3 nanocomposites. Compos Sci Technol. 2020 Oct 20;199:108323.

[12] Liu S, Li D, Yang Y, Jiang L. Fabrication, mechanical properties and failure mechanism of random and aligned nanofiber membrane with different parameters. Nanotechnol Rev. 2019 Jan;8(1):218–26.

[13] Bagheripoor M, Klassen R. Length scale plasticity: a review from the perspective of dislocation nucleation. Rev Adv Mater Sci. 2018;56(1):21–61.

[14] Lapcik L, Jindrova P, Lapcikova B. Effect of talc filler content on poly(propylene) composite mechanical properties. Proceeding paper, engineering against fracture. In: Pantelakis S, Rodopoulos C, (Eds). 1st conference on engineering against fracture conference. Patras, Greece, May 28–30, 2008. Patras: Springer Netherlands; 2009.

[15] Khan H, Amin M, Ahmad A. Characteristics of silicone composites for high voltage insulations. Rev Adv Mater Sci. 2018;56(1):91–123.

[16] Zhang P, Ling Y, Wang J, Shi Y. Bending resistance of PVA fiber reinforced cementitious composites containing nano-SiO2. Nanotechnol Rev. 2019 Jan;8(1):690–8.

[17] Pelto J, Heino V, Karttunen M, Rytoluoto I, Ronkainen H. Tribological performance of high density polyethylene (HDPE) composites with low nanofiller loading. Wear. 2020 Nov 15;460:203451.

[18] Beesetty P, Kale A, Patil B, Doddamani M. Mechanical behavior of additively manufactured nanoclay/HDPE nanocomposites. Compos Struct. 2020 Sep 1;247:112442.

[19] Lopez-Gonzalez M, Flores A, Marra F, Ellis G, Gomez-Fatou M, Salavagione J, et al. Graphene and polyethylene: a strong combination towards multifunctional nanocomposites. Polymers. 2020 Sep;12(9):2094.

[20] Privalko E, Pedosenko A, Privalko V, Walter R, Friedrich K. Composition-dependent properties of Polyethylene Kaolin composites. I. Degree of crystallinity and melting behavior of polyethylene. J Appl Polym Sci. 1999 Aug 15;73(7):1267–71.

[21] Privalko V, Sukhorukov D, Privalko E, Walter R, Friedrich K, Calleja F. Composition-dependent properties of polyethylene Kaolin composites. III. Thermoelastic behavior of injection molded samples. J Appl Polym Sci. 1999 Aug 8;73(6):1041–8.

[22] Privalko V, Korskanov V, Privalko E, Walter R, Friedrich K. Composition-dependent properties of polyethylene/kaolin composites - VI. Thermoelastic behavior in the melt state. J Therm Anal Calorim. 2000;59(1–2):509–16.

[23] Li Y, Sio W, Yang T, Tsai Y. A constitutive model of high-early-strength cement with perlite powder as a thermal-insulating material confined by caron fiber reinforced plastics at elevated temperatures. Polymers. 2020 Oct;12(10):2369.

[24] Celik AG, Kilic AM, Cakal GO. Expanded perlite aggregate characterization for use as a lightweight construction raw material. Phys Chem Probl Miner Process. 2013;49(2):689–700.

[25] Karaca E, Omeroglu S, Akcam O. Investigation of the effects of perlite additive on some comfort and acoustical properties of polyester fabrics. J Appl Polym Sci. 2016 Apr 20;133(16):43128.

[26] Ladeira NE, de Melo Furtado JG, Pacheco EBAV. Thermomorphological analysis of Al2O3/HDPE nanocomposites: one approach in function of the processing and vinyltrimethoxysilane (VTMS) content. Polym Eng Sci. 2019 Jul;59(7):1332–43.

[27] Lapcik L, Jindrova P, Lapcikova B, Tamblyn R, Greenwood R, Rowson N. Effect of the talc filler content on the mechanical properties of polypropylene composites. J Appl Polym Sci. 2008 Dec 5;110(5):2742–7.

[28] da Silva A, Rocha M, Moraes M, Valente C, Coutinho F. Mechanical and rheological properties of composites based on polyolefin and mineral additives. Polym Test. 2002 Feb;21(1):57–60.

[29] Zhang Y, Shi J, Zheng J. A method of fracture toughness JIC measurement based on digital image correlation and acoustic emission technique. Mater Des. 2021;197.

[30] Lapcik L, Vasina M, Lapcikova B, Hui D, Otyepkova E, Greenwood RW, et al. Materials characterization of advanced fillers for composites engineering applications. Nanotechnol Rev. 2019 Jan;8(1):503–12.

[31] Lapčík L, Maňas D, Vašina M, Lapčíková B, Řezníček M, Zádrapa P. High density poly(ethylene)/CaCO3 hollow spheres

composites for technical applications. Compos Part B Eng. 2017 Mar 15;113:218–24.
[32] Ehrenstein GW, Riedel G, Trawiel P. Thermal analysis of plastics: theory and practice. Munich: Carl Hanser Verlag; 2004.
[33] Cuadri AA, Martin-Alfonso JE. The effect of thermal and thermo-oxidative degradation conditions on rheological, chemical and thermal properties of HDPE. Polym Degrad Stab. 2017 Jul;141:11–8.
[34] Schawe JEK. Elastomers Vol 1. Mettler-Toledo collected applications. Schwerzenbach: Mettler-Toledo; 2002.
[35] Lapcik L, Manas D, Lapcikova B, Vasina M, Stanek M, Cepe K, et al. Effect of filler particle shape on plastic-elastic mechanical behavior of high density poly(ethylene)/mica and poly (ethylene)/wollastonite composites. Compos Part B Eng. 2018 May 15;141:92–9.
[36] Rao SS. Mechanical vibrations, 5th edn. Upper Saddle River, USA: Prentice Hall; 2010.
[37] Carrella A, Brennan MJ, Waters TP, Lopes V. Force and displacement transmissibility of a nonlinear isolator with high-static-low-dynamic-stiffness. Int J Mech Sci. 2012 Feb;55(1):22–9.
[38] Ab Latif N, Rus AZM. Vibration transmissibility study of high density solid waste biopolymer foam. J Mech Eng Sci. 2014;6:772–81.
[39] Liu K, Liu J. The damped dynamic vibration absorbers: revisited and new result. J Sound Vibrat. 2005 Jun 21;284(3–5):1181–9.
[40] Hadas Z, Ondrusek C. Nonlinear spring-less electromagnetic vibration energy harvesting system. Eur Phys J Spec Top. 2015 Nov;224(14–15):2881–96.
[41] Sun X, Zhang J. Displacement transmissibility characteristics of harmonically base excited damper isolators with mixed viscous damping. Shock Vibrat. 2013;20(5):921–31.
[42] Tang B, Brennan MJ. A comparison of two nonlinear damping mechanisms in a vibration isolator. J Sound Vibrat. 2013 Feb 4;332(3):510–20.
[43] Lapcik L, Cetkovsky V, Lapcikova B, Vasut S. Materials for noise and vibration attenuation. Chem Listy. 2000;94(2):117–22.
[44] Vasina M, Hughes DC, Horoshenkov KV, Lapcik L. The acoustical properties of consolidated expanded clay granulates. Appl Acoust. 2006 Aug;67(8):787–96.
[45] Tu Z, Shim V, Lim C. Plastic deformation modes in rigid polyurethane foam under static loading. Int J Solids Struct. 2001 Dec;38(50–51):9267–79.
[46] Bernardo V, Laguna-Gutierrez E, Lopez-Gil A, Angel Rodriguez-Perez M. Highly anisotropic crosslinked HDPE foams with a controlled anisotropy ratio: production and characterization of the cellular structure and mechanical properties. Mater Des. 2017 Jan 15;114:83–91.
[47] Ong MY, Chow WS. Kinetics of crystallization for polypropylene/polyethylene/halloysite nanotube nanocomposites. J Thermoplast Compos Mater. 2020 Apr;33(4):451–63.